



RESVERATROL LIPID BASED NANOPARTICLES SHOW A PROMISING OUTCOME ON INDUCED NON ALCOHOLIC FATTY LIVER DISEASE

Dina Adel Abdelmalek^{1*}, Basma Nagy Abd-Elhamid¹, Noura Hassan Abd Ellah^{1,2} and Sayed Ismail¹

¹Department of Pharmaceutics, Faculty of Pharmacy, Assiut University, Assiut, Egypt

²Department of Pharmaceutics, Faculty of Pharmacy, Badr University in Assiut, Naser city, Assiut, Egypt

Prevalence of nonalcoholic fatty liver disease (NAFLD) affects more than 25% of the populations worldwide. In this study, resveratrol loaded solid lipid nanoparticles (Res-SLN) were prepared by emulsification and were in vitro evaluated. Res-SLN 1 containing gelucire and tween 80 was selected for further in vitro and in vivo studies. In vivo studies were done via induction of NAFLD in rats with a high fat (HF) diet for 12-weeks followed by a 6-week period of treatment with Res-SLN1. Blood samples and liver sections were taken from rats for biochemical and histological evaluations. Res-SLN1 exhibited high entrapment efficiency (75±22%), small particle size (208±48 nm) and an acceptable release rate. In vivo studies demonstrated a remarkable improvement in lipid profile and liver enzyme with Res-SLN1. The histological features were significantly improved with Res-SLN1. Res-SLN1 represent a promising therapeutic approach for NAFLD via prolonging Res release and ameliorating lipid profile and liver enzymes.

Keywords: Nonalcoholic fatty liver disease, resveratrol, solid lipid nanoparticles

INTRODUCTION

Non-alcoholic fatty liver disease (NAFLD) has become one of the most common chronic liver disorders and is recognized to have a close, bidirectional association with components of metabolic syndrome¹. It comprises different stages of liver pathologies, starting from simple steatosis to nonalcoholic steatohepatitis (NASH), then progressing to fibrosis, cirrhosis and hepatocellular carcinoma². NAFLD is usually associated with obesity, insulin resistance, type 2 diabetes mellitus, hypertension and dyslipidemia³. Unhealthy habits such as an increased intake of carbohydrates and saturated fats and a sedentary daily attitude are considered important causes of NAFLD. Until now, there is no optimum drug treatment for NAFLD⁴. Vitamin E, statins, metformin and pioglitazone have demonstrated some benefits in the resolution of NAFLD. However, widespread

use of these drugs has been limited by concerns over potential risks of long-term treatment such as weight gain, stroke, and prostate cancer. The optimal pharmacotherapy for NAFLD remains uncertain⁵.

Resveratrol (Res) (3, 5, 4/-trihydroxy-trans-stilbene) is a naturally occurring active biomolecule, which belongs to the polyphenol family⁶. It is a non-flavonoid polyphenol and it is mainly found in grapes, berries and nuts. The role of Res in the management of NAFLD, metabolic syndrome and type II diabetes mellitus has been related to its antioxidant and anti-inflammatory effect⁷. Moreover other studies spotted a noticeable effect of Res on regulating lipid metabolism and modulating apoptosis⁸.

Like most polyphenols, Res exhibits some troublesome properties such as limited water solubility, low bioavailability, low oxidative stability and photosensitivity that constrain its use in pharmacotherapy and limits its efficacy

when administered via conventional dosage forms⁹. It has been widely recognized that the use of appropriate nano-delivery systems is one of the most effective strategies to overcome the therapeutic limitations of polyphenolic compounds. Among all the reported nano-delivery systems for phytochemicals, lipid-based nanocarriers seem to be one of the most appropriate delivery systems for hydrophobic or lipid-soluble compounds, due to their biocompatibility with lipid matrices¹⁰. Solid lipid nanoparticles (SLNs), as drug carriers, have been confirmed to exhibit many advantageous features including non-toxicity, biocompatibility, high stability, prolonged drug release and high bioavailability over traditional colloidal delivery systems¹¹. The present study aims to establish a solid lipid nanocarrier for Res and assess its role in improving of induced NAFLD as tested *in vivo* using a rat model.

MATERIALS AND METHODS

Materials

Res was purchased from AK Scientific Inc. (California, USA). Tween® 80 was purchased from Sigma Aldrich, Inc. (St. Louis, USA). Precirol® ATO 5 and Gelucire® 50/13 were provided as gifts by Gattefossé SAS (Saint-Priest, France). Biochemical kits for Triglyceride (TG), total cholesterol (TC), low-density lipoprotein cholesterol (LDL), alanine transaminase (ALT), alkaline phosphatase (ALP), and aspartate aminotransferase (AST) were purchased from Biodiagnostic Company (Giza, Egypt) and used according to the manufacturer's instructions. All other reagents were of pharmaceutical grade.

Preparation of resveratrol loaded solid lipid nanoparticles (Res-SLNs)

Res-SLNs were prepared by the emulsification method¹². Two formulations were prepared: Res-SLN1, which was composed of Gelucire® 50/13 as the solid lipid and Res-SLN2, which was composed of Precirol® ATO 5 as the solid lipid. In both formulations Tween 80 (5% w/v) was used as the surfactant. All the other formulation variables were kept constant. The solid lipid (1.5 g which corresponds to 5% w/v) was heated to a temperature 5–10°C above its melting point (50°C for gelucire and 55°C for precirol) forming the lipid phase. 20 mg of Res was added to the lipid phase. An aqueous phase

was prepared by dissolving 1.5 g of Tween 80 in distilled water to form a final concentration of 5% (w/v). The aqueous phase (30 mL) was heated to the same temperature as the lipid phase (60°C). The hot aqueous phase is then added to the molten lipid phase under magnetic stirring; this stage produces a hot coarse o/w emulsion. Further particle size reduction was achieved via a homogenizer (Bio-Gen PRO200, Connecticut, USA) at 21000 rpm for 20 min. The obtained formulation was stored overnight in the fridge until further characterization.

Determination of mean particle size, polydispersity index (PDI) and zeta potential

The mean particle size, polydispersity index (PDI) and zeta potential of Res-SLNs were determined using the Malvern® Zetasizer Nano ZS90 (Malvern® Instruments Limited, UK) at 25°C. Before measurement, samples were diluted with distilled water and vortexed for 1 min. Measurements were performed in triplicate using a 90° scattering angle.

Determination of entrapment efficiency (EE)

To determine EE, dialysis bag method was used¹³. This method allows direct measurement of EE and is based on the idea of separating the untrapped drug from the drug entrapped in SLN via a dialysis bag instead of centrifugation^{14,15}. A certain volume of the formulation (0.5 mL) was placed inside the dialysis bag (Mwt cut-off: 12–14 kDa) to be placed in a beaker containing distilled water (100 mL). The system was allowed to stir on the magnetic stirrer for 2 h. This time is sufficient to allow the free Res to diffuse out of the dialysis bag to the dialysis medium (distilled water). Afterwards, the content inside the dialysis bag was collected and 200 µl was withdrawn and added to a 10 ml chloroform/methanol mixture (1:4) in order to digest the lipids and allow the drug to be released. Res content was determined spectrophotometrically (Shimadzu, the model UV-1800 PC, Kyoto, Japan) at $\lambda_{max} = 305$ nm against blank SLNs by the following equation:

$$EE(\%) = \frac{\text{measured Res content in SLNs}}{\text{theoretical content of Res in SLNs}} \times 100$$

Differential scanning calorimetry (DSC)

DSC patterns were conducted for pure Res, gelucire 50/13, freeze dried blank SLNs and Res-SLNs using Shimadzu DSC TA-50 ESI DSC apparatus (Tokyo, Japan) at a scanning rate of 10 °C/min from 30°C to 350°C under a nitrogen gas stream at a flow rate of 40 ml/min using 4–8 mg of sample.

Fourier-Transform Infrared Spectroscopy (FT-IR)

FT-IR spectra of Res, gelucire 50/13, freeze dried blank SLNs and Res-SLNs were recorded on a Thermo Scientific™ Nicolet™ iS-50 Fourier-transform infrared spectrometer sample holder and subjected to FT-IR spectroscopy in the wavelength region between 4000 and 500 cm⁻¹ with 4 cm⁻¹ resolution. The absorbance and intensity of the characteristic peaks for the aforementioned samples in spectral regions of interest were identified and recorded.

***In vitro* drug release study**

Dialysis bag method was used to determine cumulative drug released in different release media (phosphate buffer saline (PBS, pH 7.4), simulated gastric fluid without pepsin (pH 1.2) and enzyme-free simulated intestinal fluid (pH 6.8)¹⁶. Res-SLNs (1 mL) were placed in the dialysis membrane, which was sealed from both ends and put in a beaker containing 100 mL of release medium. The system was maintained for 48 hrs at 37°C in a thermostatically controlled shaker water bath at 50 rpm (Gesellschaft Labor Technik M.B.H. &Co., GFL, Germany). Samples (5 mL) were withdrawn at predetermined time intervals and replaced with fresh medium. The released drug was measured spectrophotometrically (λ max =305nm). The release experiment was run in triplicate against a blank formulation similarly treated.

Morphology of Res-SLNs

The morphology of selected Res-SLNs was observed by transmission electron microscopy (TEM; JEOL JEM-1010S, Tokyo, Japan). Formulation was placed on a carbon-coated copper grid and the excess was removed. After drying on the grid, the sample was observed by TEM and photographed.

***In vivo* study**

The experiment was carried out on 18 Sprague-Dawley male rats (200 ± 20 g). Rats were randomly assigned to the study and then separated into plastic cages. The rats were kept in 12 h light/dark cycles in temperature-controlled rooms and they had ad libitum access to food and water. Rats had one week of acclimatization before the experiment. Rats were divided into three groups: a negative control group (Group I) that received a standard chow diet, a high-fat diet, (HF) group (Group II) that received a high fat diet for 12 weeks and a treated group (Group III) that received a high fat diet for 12 weeks followed by treatment with the selected Res-SLNs (20mg/kg/day, p.o.) for 6 weeks. High-fat diet was prepared by adding 30–40% butter fat and 1% cholesterol to standard chow diet¹⁷. The high-fat diet, which had 50% fat compared to the standard chow diet (only 10 % fat), was freshly prepared every 3 days and kept at 4°C. At the end of the experiment, the rats were fasted for 12 h prior to sacrifice and the procedure was conducted under deep phenobarbital anesthesia. Animal experiments were approved by the Local Ethical Committee on Animal Testing in Assiut, Faculty of Medicine (**approval No. 17200772 dated 11/10/2022**).

Biochemical Analysis

4 mL of blood was collected from the retro-orbital plexus of rats using a heparinized capillary tube and a clean dried centrifuge tube. After 20 min, the blood was centrifuged for 15 min at 4 °C and 3000 rpm. Serum was quickly collected and frozen at -20 °C until biochemical analysis. Triglyceride (TG), total cholesterol (TC), low-density lipoprotein cholesterol (LDL), alanine transaminase (ALT), alkaline phosphatase (ALP), and aspartate aminotransferase (AST) were assayed spectrophotometrically (Jenway, UV-6305, Ltd.; Fesltd, Dunmow, UK).

Histological study

Histological investigations were conducted to confirm the biochemically associated changes. After the sacrifice of the rats, their livers were extracted, and inspected. Portions of the liver from the left lateral lobe were dissected and processed for light microscopic examinations.

Fixed liver samples were processed in the Zoology Department, Faculty of Science, Assiut University, according to standard staining procedures. A piece of the left lateral lobe of the liver was taken and immediately fixed in 10% buffered formaldehyde for 24 h. The fixed specimens were then trimmed, washed and dehydrated in ascending grades of alcohol. Specimens were then cleared in xylene, embedded in paraffin, sectioned at 4-6 microns thickness, and processed to be stained with hematoxylin and eosin (H&E) for inspection of liver histoarchitectural features, and Masson trichrome for detection of liver fibrosis. Slides of liver sections were examined by a light microscope and photographed.

Statistical analysis

Data were presented as mean \pm SD and comparisons between the means were done using unpaired t-tests and one way ANOVA followed by a post hoc Tukey test using Graph Pad Prism Software version 6.0 (USA), where $p \leq 0.05$ was considered statistically significant.

RESULTS AND DISCUSSION

Results

Preparation of Res-SLNs

The emulsification method followed by homogenization was carefully chosen for the preparation of SLNs as it is a reliable, simple, and reproducible method without fearing from the incomplete evaporation of organic solvents in other preparation methods¹⁸. Selection of a suitable lipid and surfactant was based on two major criteria: maximizing entrapment and minimizing particle size. Preliminary studies were done using different lipids such as compritol 888, geleol, precirol ATO5 and gelucire 50/13 at different concentrations (unpublished data). It was observed that precirol ATO5 and gelucire 50/13 (at 5% w/v) displayed higher EE amongst the other lipids and concentrations. Tween 80 was used at a

concentration of 5% w/v, which demonstrated acceptable stabilization of the formulated SLNs. Accordingly; two formulations of SLNs were selected for further *in vitro* characterization.

In vitro characterization of Res- SLNs

In vitro characterization parameters of the two fabricated Res-SLNs are shown in (Table 1). The only difference in the two formulations was in the lipid type while all the other variables were kept constant. First of all, the study revealed that the lipid type had a significant effect on particle size with Precirol ATO5 yielding larger nanoparticles (304 ± 28 nm) compared to SLNs prepared using gelucire 50/13 (208 ± 48 nm). This might be attributed to the lower melting point of the former leading to less viscosity of the molten lipid phase, leading to smaller size¹⁹. Res-SLN 2 showed non-significant lower EE than Res SLN 1. Gelucire is composed of a diverse structure of fatty acids which imparts disorder in the lipoidal structure thereby providing spaces for active compound accommodation²⁰.

Finally Res-SLN 1 depicted lower PDI values than that of Res-SLN2 and the zeta potential did not significantly vary between the two SLNs showing a high negative surface charge. The negative sign could be attributed to the free fatty acid present on SLN surface. Nonionic surfactants do not confer charge to the particle but sterically stabilizes the SLN by forming a coat around their surface. In addition, presence of gelucire, a hydrophilic lipid, could have helped in the formation of solvent sheath and imparted rigidity to interface due to formation of hydrogen bonds with the surrounding aqueous phase²¹. Accordingly, Res-SLN1 was chosen for further *in vitro* and *in vivo* studies.

Table 1: Characterization of the two prepared Res-SLNs.

Formulation	Particle size (nm)	Zeta potential (mV)	PDI	EE (%)
Res-SLN1	208 ± 48	-18 ± 3	0.355 ± 0.01	75.7 ± 22
Res-SLN2	304 ± 28	-22.4 ± 0.4	0.516 ± 0.11	70.3 ± 4

Differential scanning calorimetry (DSC)

The DSC thermogram of Res showed a sharp endothermic peak at 268°C, corresponding to its melting point (Fig. 1). At 44 °C, a peak was observed owing to the melting point of gelucire 50/13. Both the Res-SLN1 and the blank SLNs showed quite similar thermograms, with the drug peak disappearing in Res-SLN1. This may be due to the incorporation of the drug into the lipid matrix²². Previous studies have postulated that the disappearance of the drug peak in the prepared SLNs could be a result of the solubilization of the drug in the lipid phase⁶ or the conversion of the drug from the crystalline state to a molecularly dispersed amorphous state within the nanoparticle formulations²³.

Fourier-Transform Infrared Spectroscopy (FT-IR)

The IR spectra of different components of SLNs, blank SLN1 and Res- SLN1, are shown in (Fig. 2). The IR spectrum of pure Res shows a broad band at 3239.2 cm⁻¹, corresponding to OH stretching of the phenolic group with intermolecular H bonding and a sharp band at 1606 cm⁻¹, indicating C=C stretching of the aromatic ring. As for gelucire 50/13, it shows a broad band at 3350 cm⁻¹, correlating with O-H and forked band for N-H stretching at 3000 cm⁻¹. Comparing the spectra of blank SLN1 and Res-SLN1, it can be deduced that the vibration bands from 500 cm⁻¹ to 1750 cm⁻¹ are quite similar, with the absence of new peaks indicating no clear interaction between Res and the components²⁴.

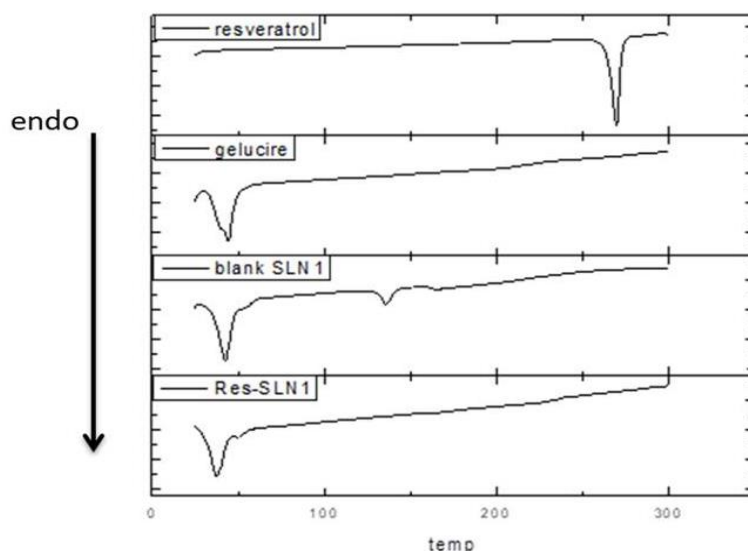


Fig. 1: DSC thermograms of Res, gelucire, balnk SLN1 and Res-SLN1.

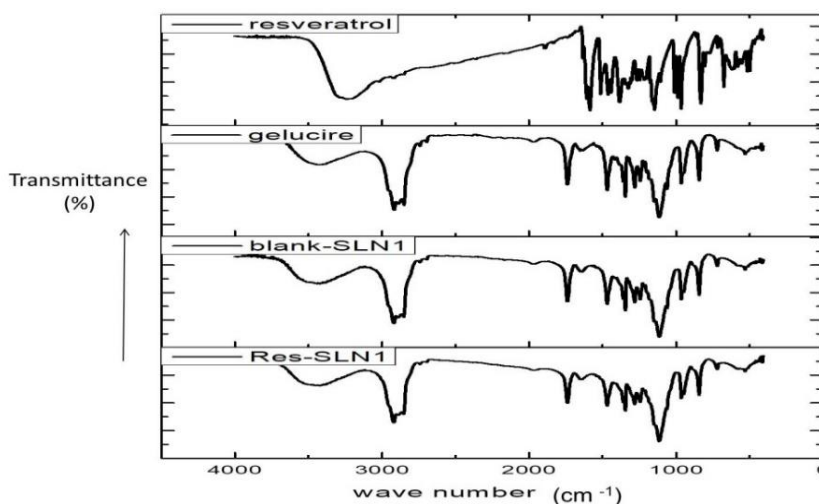


Fig. 2: FT-IR spectra of Res, gelucire, blank SLN1 and Res-SLN1.

***In vitro* drug release study**

The *in vitro* release profile of Res-SLN1 was conducted in simulated gastric fluid (pH 1.2) (**Fig. 3a**), simulated intestinal fluid (pH 6.8) (**Fig. 3b**) and phosphate buffer saline (pH 7.4) (**Fig. 3c**). At pH 1.2, it is noticed that the SLNs released less than 20% of Res after 2 h, which is the expected resident time of the SLNs in the stomach. This implies that the lipid nanoparticles are able to remain intact within the stomach with a small percent of Res released. At pH 6.8, the release of Res was around 40% after 12 h. A similar profile was seen at pH 7.4, where the cumulative % of drug released after 48 h was 42%. SLNs are well known to exhibit a biphasic release profile with an initial burst release that occurs due to the diffusion of the drug that is allocated in the outer surfactant layer, followed by sustained release owing to the diffusion of the drug from the lipid core²⁵. The sustained release effect

seen in Res-SLN1 may be due to the large amount of lipoidal core that solubilizes the drug and keeps it dwelling within the lipid matrix of the SLN. High concentration of the lipid phase (5% w/v) yields more rigid solidified nanoparticles, which would also slow down the drug diffusion to the dissolution medium²⁶. This goes in concordance with the study conducted by Cho *et al.*²⁷, who observed that at pH 7.4, the release of docetaxel from SLN after 24 hours was only about 40%, and this was attributed to the slow diffusion of the drug from the lipid core.

Morphology of Res-SLNs

The formulated Res-SLN1 showed a nearly spherical structure (**Fig. 4**), which is in concordance with several reported studies revealing that most SLNs appear as spherical or nearly spherical structures in conventional TEM²⁸.

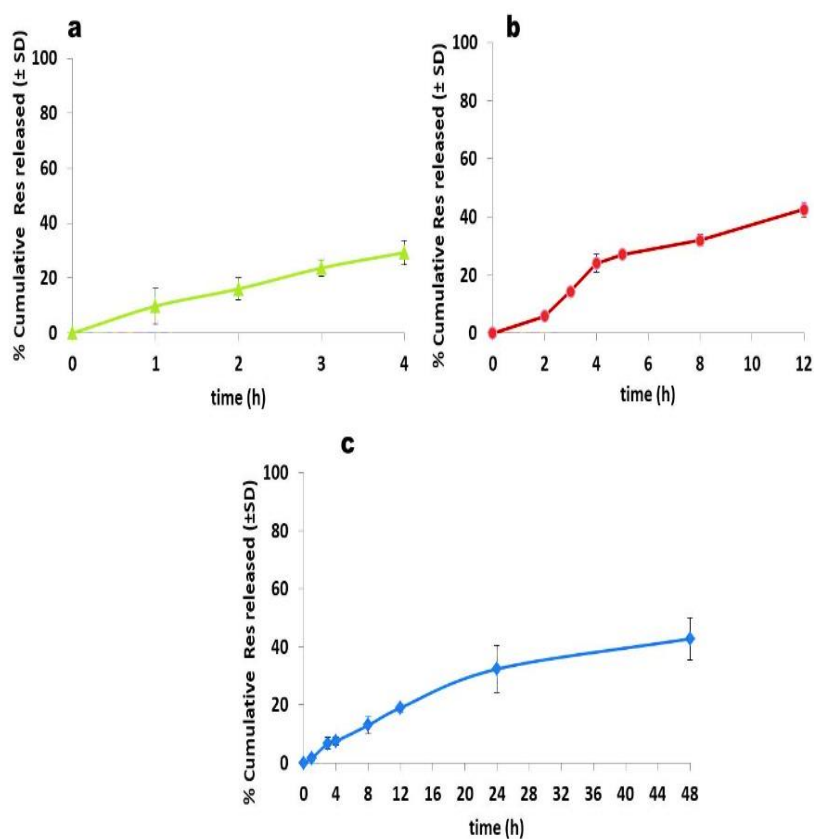


Fig. 3: *In vitro* release profile of Res-SLN1 in different release media: (a) pH 1.2. (b) pH 6.8 and (c) pH 7.4. (Data are represented as mean of triplicate values of cumulative % of Res released ± SD,).

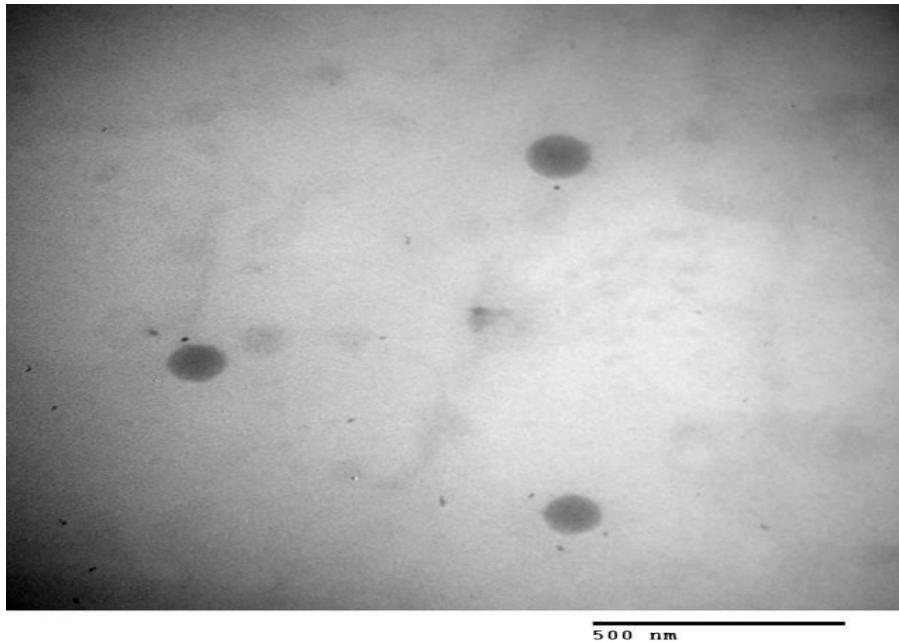


Fig. 4: Transmission electron microscope (TEM) image of Res-SLN1 (bar=500nm).

***In vivo* study**

Biochemical Analysis

Serum lipid profile and liver enzymes

NAFLD is closely associated with metabolic disorders, including central obesity, dyslipidemia, hypertension, hyperglycemia and persistent abnormalities of liver function tests. Measuring serum lipid profile and liver enzymes would be a primary noninvasive indicator of the possible development of this disease²⁹. In this study, it was observed that rats fed a high fat (HF) diet depicted a significant increase in TC, TG and LDL (**Fig. 5a-c**) compared to the control group. Interestingly, Res-SLN1s were able to induce a significant drop in the aforementioned parameters (TC, TG and LDL).

Similar effects were seen in liver enzymes. The group treated with Res-SLN1 revealed a significant decrease in liver enzymes (ALT, AST and ALP) compared to that of the HF group (**Fig. 5d-f**) returning back to almost normal values of the control group. Res has been reported to have significant effects on lipid metabolism. Previous research work has suggested that this may be due reduced fat accumulation either in isolated adipocytes or in adipose tissue and liver, increased fatty acid oxidation in skeletal muscle and reduced serum lipids induced by this polyphenol³⁰. Moreover, this effect could be further improved as the drug is loaded in SLNs. This is because, unlike most other tissues, the liver does not exhibit an

impermeable basal lamina. Hence, in the absence of interfering mechanisms such as aggregation or protein binding, the majority of nanoparticles with an approximate size of 200 nm exhibit rapid passive liver accumulation of the drug following systemic administration³¹.

Histological study

Based on the histological observation of the liver sections stained with hematoxylin and eosin (H&E), the control group displayed regular cellular morphology, distinct hepatocytes, no lipid accumulation, and no histological abnormalities (**Fig. 6a**). In contrast, the liver tissues of the HF group exhibited extensive cytoplasmic vacuole formation and ballooning, together with disorientation in the liver cords. The fat vacuoles appeared intracellularly, pushing the nucleus towards the edge of the cell, forming what is known as a signet ring appearance (**Fig. 6c**). Additionally, inflammatory cell infiltration was noticed in the photomicrograph of the HF group (**Fig. 6d**). This reveals that induced NAFLD has progressed from the initial stage of steatosis to steatohepatitis³². Fibrosis was seen prominently in the HF group (**Fig. 6e**), as indicated by a strong positive green reaction of Masson trichrome stain, as opposed to minimal appearance of collagen fibers in the control group (**Fig. 6b**). This goes in agreement with Maciejewska et al.³³, who stated that the stage

of liver fibrosis begins to appear after 12 weeks of administration of HF diet.

After a six-week treatment with Res-SLN1, the third group of rats starts to show an improvement in liver architecture and orientation in liver cords and a decrease in hepatocyte ballooning when compared to the HF group ((**Fig. 6f**). Furthermore, this group has shown a decrease in fibrosis ((**Fig. 6g**) in comparison with the HF group. Previous studies have suggested that Res has shown a positive effect in attenuating induced NAFLD^{30&34}, and this effect was attributed to its strong antioxidant abilities and its effect on fat oxidation and metabolism³⁵. However, its use has been constrained by its challenging pharmacokinetic properties. The present research work focused on improving the delivery of Res to the target site (the liver) via incorporating it in SLNs, thereby maximizing

its efficacy in managing NAFLD and overcoming its limiting properties such as poor water solubility and poor bioavailability. Unlike most other tissues, liver tissue is known for containing sinusoidal fenestrae. Hence, in the absence of interfering mechanisms such as aggregation or protein binding, the majority of nanoparticles with particle sizes of around 200 nm exhibit rapid passive liver accumulation following systemic administration³¹. A study conducted by **Wang et al.**, who formulated sorafenib SLNs, supports this hypothesis. It was observed that better hepatic accumulation of sorafenib is achieved after oral administration when the drug is formulated as SLNs compared to sorafenib suspension³⁶. This could be a possible explanation for why the prepared Res-SLN1 exhibited positive outcomes in managing induced NAFLD in rats in such a short period of time (6 weeks).

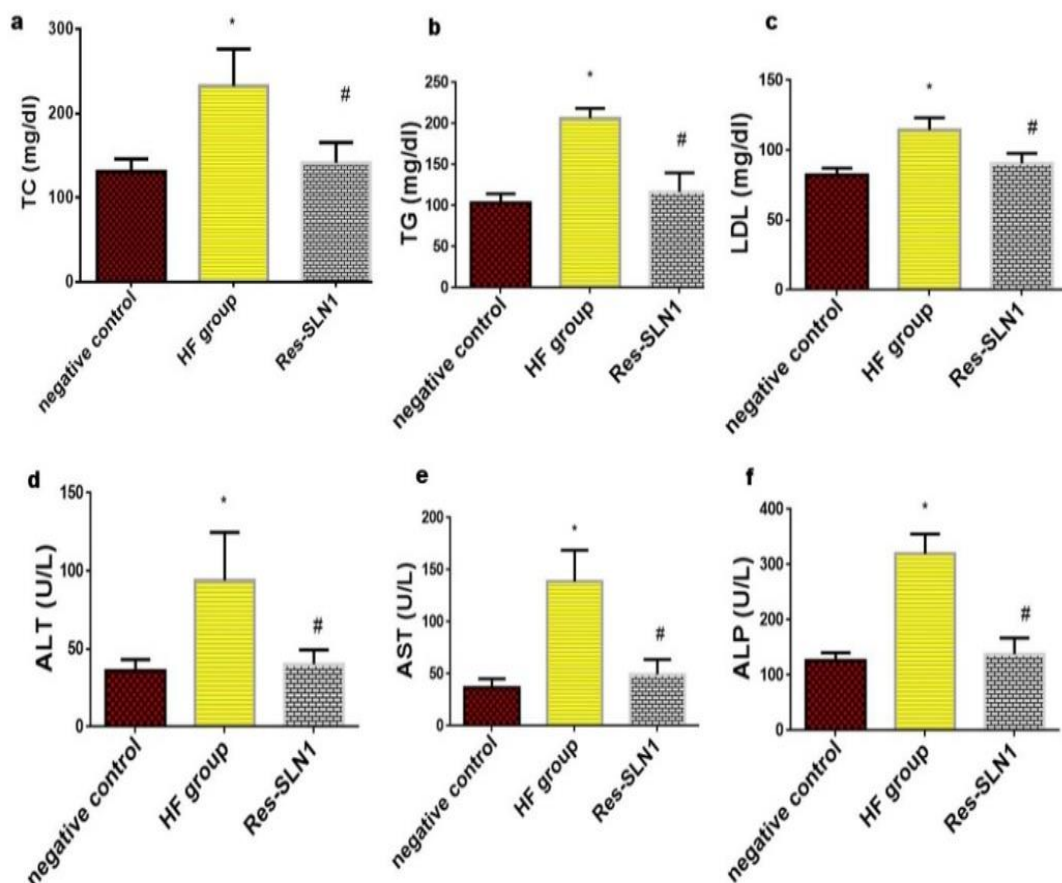


Fig. 5: Serum lipid profiles: (a) TC (total cholesterol) (b) TG (triglycerides), (c) LDL (low density lipoproteins) and values of liver enzymes: (d) ALT (alanine transaminase) AST (aspartate aminotransferase), (f) ALP (alkaline phosphatase) in studied groups. * difference is significant compared to negative control group at $p < 0.05$, #: difference is significant compared to HF group at $p < 0.05$.

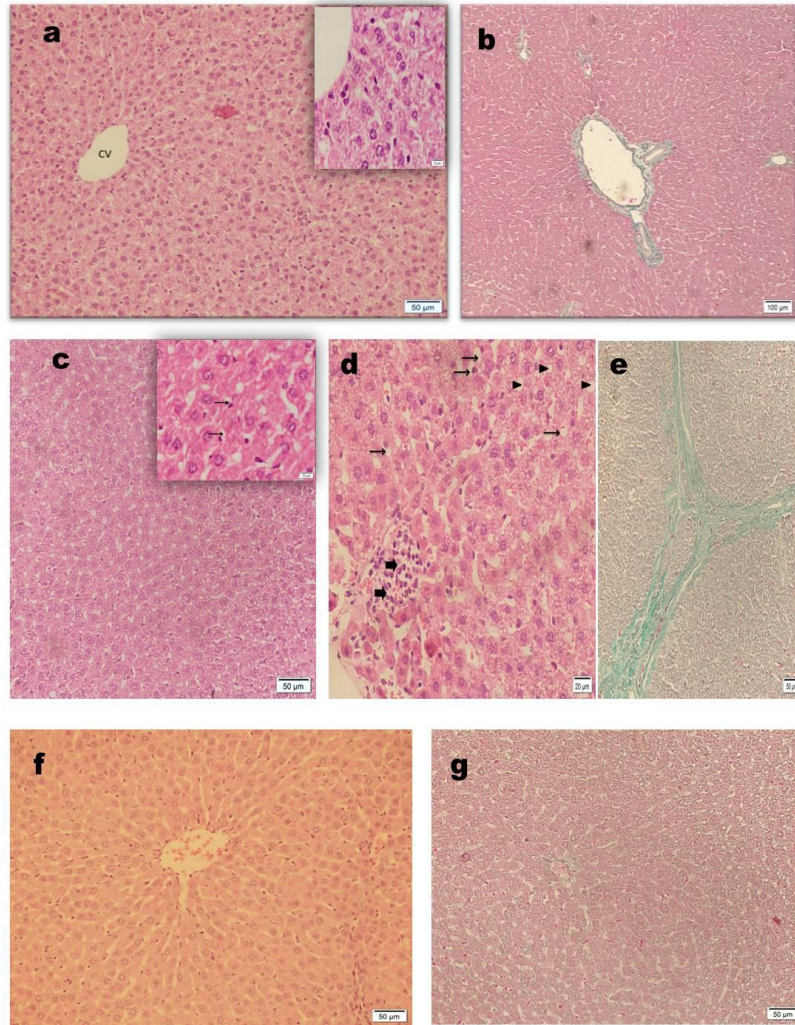


Fig. 6: Photomicrographs of the liver tissue (a) Control group showing normal liver architecture of liver lobules surrounding the central vein (CV), X200, with higher magnification on the top right, showing normal hexagonal hepatocytes containing a round vesicular nucleus (1000 X). (b) Normal liver tissue showing minimal fibrosis. X100. Masson trichrome. (c) HF group showing ballooning of hepatocytes at X200 with higher magnification at X1000 on the top right showing signet ring appearance (arrows) of liver cells. H&E. (d) HF group showing steatosis; many hepatocytes appear as a signet ring (arrows), fat vacuoles (head arrow), and inflammatory cells (short arrows) X400. H&E. (e) HF group showing prominent fibrosis X200. Masson trichrome. (f) Group III treated with Res-SLN: start to regain normal orientation of cords with less ballooning in hepatocytes X200. H&E stain. (g) Group III shows a decrease in amount of fibrosis. X200. Masson trichrom.

Conclusion

The present study aims at augmenting the efficacy of Res in mitigating the damage done to the liver cells in NAFLD. Solid lipid nanoparticles containing Res were successfully prepared using emulsification technique followed by homogenization. Res-SLN1 exhibited small particle size, high EE and a sustained release pattern at pH 7.4. The current *in vivo* studies showed impressive results in ameliorating biochemical parameters in the form of lowered serum lipid profiles and liver enzymes compared with control groups.

Moreover, the histological features that are associated with NAFLD showed significant improvement in the form of a decrease in hepatocyte ballooning and liver architecture restoration. It can be deduced that Res-SLN1 has obviously improved the overall action of Res in the treatment of NAFLD. Further research work is to be conducted to focus on exploring various formulations to achieve the most optimal lipid based nanoparticles.

Conflict of interest

The authors declare no conflict of interest.

REFERENCES

- Z. Younossi, Q.M. Anstee, M. Marietti, T. Hardy, L. Henry, M. Eslam, J. George and E. Bugianesi, "Global burden of NAFLD and NASH: trends, predictions, risk factors and prevention", *Nat Rev Gastroenterol Hepatol*, 15(1), 11-20 (2018).
- M. Theodotou, K. Fokianos, D. Moniatis, R. Kadlenic, A. Chrysikou, A. Aristotelous, A. Mouzouridou, J. Diakides and E. Stavrou, "Effect of resveratrol on non-alcoholic fatty liver disease", *Exp Ther Med*, 18(1), 559-565 (2019).
- E.E. Powell, V.W.-S. Wong and M. Rinella, "Non-alcoholic fatty liver disease", *The Lancet*, 397(10290), 2212-2224 (2021).
- X. Yin, X. Guo, Z. Liu and J. Wang, "Advances in the Diagnosis and Treatment of Non-Alcoholic Fatty Liver Disease", *Int J Mol Sci*, 24(3), 2844 (2023).
- R. Paternostro and M. Trauner, "Current treatment of non-alcoholic fatty liver disease", *J Intern Med*, 292(2), 190-204 (2022).
- E.H. Gokce, E. Korkmaz, E. Deller, G. Sandri, M.C. Bonferoni and O. Ozer, "Resveratrol-loaded solid lipid nanoparticles versus nanostructured lipid carriers: evaluation of antioxidant potential for dermal applications", *Int J Nanomedicine*, 7 1841-1850 (2012).
- S. Wan, L. Zhang, Y. Quan and K. Wei, "Resveratrol-loaded PLGA nanoparticles: enhanced stability, solubility and bioactivity of resveratrol for non-alcoholic fatty liver disease therapy", *R Soc Open Sci*, 5(11), 181457 (2018).
- M. Karimi, B. Abiri, P.C. Guest and M. Vafa, "Therapeutic Effects of Resveratrol on Nonalcoholic Fatty Liver Disease Through Inflammatory, Oxidative Stress, Metabolic, and Epigenetic Modifications, in: P.C. Guest (Ed.) Physical Exercise and Natural and Synthetic Products in Health and Disease", *Springer US New York NY*, 19-35 (2022).
- P. Devi, P. Sharma, C. Rathore and P. Negi, "Novel Drug Delivery Systems of Resveratrol to Bioavailability and Therapeutic Effects, in: Resveratrol-Adding Life to Years", *Not Adding Years to Life, IntechOpen*, (2019).
- D.Q. Falcão, A.P. Oliveira, B.G. Lima, A.C. Cardoso, K.B. Almeida, T.C. Santos, L.M. Nascimento, G.C. Desmarais, P.S. Sanches and E.M. Araújo, "Nanotechnology in phytotherapy: current challenges of lipid-based nanocarriers for the delivery of natural products, in: Lipid Nanocarriers for Drug Targeting", *Elsevier*, 139-174 (2018).
- C.-H. Tang, H.-L. Chen and J.-R. Dong, "Solid Lipid Nanoparticles (SLNs) and Nanostructured Lipid Carriers (NLCs) as Food-Grade Nanovehicles for Hydrophobic Nutraceuticals or Bioactives", *Applied Sciences*, 13(3), 1726 (2023).
- I.A. Elbahwy, H.M. Ibrahim, H.R. Ismael and A.A. Kasem, "Enhancing bioavailability and controlling the release of glibenclamide from optimized solid lipid nanoparticles", *J Drug Deliv Sci Technol*, 38, 78-89(2017).
- S. Daneshmand, S. Golmohammadzadeh, M.R. Jaafari, J. Movaffagh, M. Rezaee, A. Sahebkar and B. Malaek-Nikouei, "Encapsulation challenges, the substantial issue in solid lipid nanoparticles characterization", *J Cell Biochem*, 119(6), 4251-4264 (2018).
- N.K. Swarnakar, K. Thanki and S. Jain, "Bicontinuous cubic liquid crystalline nanoparticles for oral delivery of doxorubicin: implications on bioavailability, therapeutic efficacy, and cardiotoxicity", *Pharm Res*, 31(5), 1219-1238 (2014).
- S. Khurana, P. Bedi and N. Jain, "Development of nanostructured lipid carriers for controlled delivery of mefenamic acid", *International Journal of Biomedical Nanoscience and Nanotechnology*, 2(3-4), 232-250 (2012).
- V. Piazzini, B. Lemmi, M. D'Ambrosio, L. Cinci, C. Luceri, A.R. Bilia and M.C. Bergonzi, "Nanostructured lipid carriers as promising delivery systems for plant extracts: The case of silymarin", *Appl Sci*, 8(7), 1163 (2018).

17. M. Balbaa, M. El-Zeftawy, D. Ghareeb, N. Taha and A.W. Mandour, "Nigella sativa relieves the altered insulin receptor signaling in streptozotocin-induced diabetic rats fed with a high-fat diet", *Oxid Med Cell Longev*, 2016, 2492107 (2016).
18. B. Subramaniam, Z.H. Siddik and N.H. Nagoor, "Optimization of nanostructured lipid carriers: Understanding the types, designs, and parameters in the process of formulations", *J Nanopart Res*, 22, 1-29 (2020).
19. A. Gumireddy, R. Christman, D. Kumari, A. Tiwari, E.J. North and H. Chauhan, "Preparation, characterization, and in vitro evaluation of curcumin-and resveratrol-loaded solid lipid nanoparticles", *AAPS PharmSciTech*, 20, 1-14 (2019).
20. M.-J. Tsai, P.-C. Wu, Y.-B. Huang, J.-S. Chang, C.-L. Lin, Y.-H. Tsai and J.-Y. Fang, "Baicalein loaded in tocol nanostructured lipid carriers (tocol NLCs) for enhanced stability and brain targeting", *Int J Pharm*, 423(2), 461-470 (2012).
21. S.S. Deshkar, S.G. Bhalerao, M.S. Jadhav and S.V. Shirolkar, "Formulation and optimization of topical solid lipid nanoparticles based gel of dapsone using design of experiment", *Pharm Nanotechnol*, 6(4), 264-275 (2018).
22. M.A. Kalam, Y. Sultana, A. Ali, M. Aqil, A.K. Mishra, I.A. Aljuffali, A. Alshamsan, Part I: Development and optimization of solid-lipid nanoparticles using Box- Behnken statistical design for ocular delivery of gatifloxacin", *J Biomed Mater Res A*, 101, 1813-1827 (2013).
23. A. Vijayakumar, R. Baskaran, Y.S. Jang, S.H. Oh and B.K. Yoo, "Quercetin-loaded solid lipid nanoparticle dispersion with improved physicochemical properties and cellular uptake", *AAPS Pharm Sci Tech*, 18, 875-883 (2017).
24. P. Ramalingam and Y.T. Ko, "Improved oral delivery of resveratrol from N-trimethyl chitosan-g-palmitic acid surface-modified solid lipid nanoparticles", *Colloids Surf B*, 139, 52-61 (2016).
25. C. Senthil Kumar, R. Thangam, S.A. Mary, P.R. Kannan, G. Arun and B. Madhan, "Targeted delivery and apoptosis induction of trans-resveratrol-ferulic acid loaded chitosan coated folic acid conjugate solid lipid nanoparticles in colon cancer cells", *Carbohydr Polym*, 231, 115682 (2020).
26. N. Badawi, K. El-Say, D. Attia, M. El-Nabarawi, M. Elmazar and M. Teaima, "Development of Pomegranate Extract-Loaded Solid Lipid Nanoparticles: Quality by Design Approach to Screen the Variables Affecting the Quality Attributes and Characterization", *ACS Omega*, (2020).
27. H.-J. Cho, J.W. Park, I.-S. Yoon and D.-D. Kim, "Surface-modified solid lipid nanoparticles for oral delivery of docetaxel: enhanced intestinal absorption and lymphatic uptake", *Int J Nanomedicine*, 9, 495 (2014).
28. A. Gordillo-Galeano and C.E. Mora-Huertas, "Solid lipid nanoparticles and nanostructured lipid carriers: A review emphasizing on particle structure and drug release", *Eur J Pharm Biopharm*, 133, 285-308 (2018).
29. S. Pouwels, N. Sakran, Y. Graham, A. Leal, T. Pintar, W. Yang, R. Kassir, R. Singhal, K. Mahawar and D. Ramnarain, "Non-alcoholic fatty liver disease (NAFLD): a review of pathophysiology, clinical management and effects of weight loss", *BMC Endocr Disord*, 22, 63 (2022).
30. S. Gómez-Zorita, A. Fernández-Quintela, M. Macarulla, L. Aguirre, E. Hijona, L. Bujanda, F. Milagro, J. Martínez and M. Portillo, "Resveratrol attenuates steatosis in obese Zucker rats by decreasing fatty acid availability and reducing oxidative stress", *Br J Nutr*, 107(2), 202-210 (2012).
31. R. Böttger, G. Pauli, P.-H. Chao, N. Al Fayez, L. Hohenwarter and S.-D. Li, "Lipid-based nanoparticle technologies for liver targeting", *Adv Drug Deliv Rev*, 154-155 79-101 (2020).
32. T. Karatzas, N. Sikalias, D. Mantas, A. Papalois, K. Alexiou, L. Mountzalia and G. Kouraklis, "Histopathological changes and onset of severe hepatic steatosis in rats fed a choline-free diet", *Exp Ther Med*, 16(3), 1735-1742 (2018).

33. D. Maciejewska, A. Łukomska, K. Dec, K. Skonieczna-Żydecka, I. Gutowska, M. Skórka-Majewicz, D. Styburski, K. Misiakiewicz-Has, A. Pilutin and J. Palma, "Diet-induced rat model of gradual development of non-alcoholic fatty liver disease (NAFLD) with lipopolysaccharides (LPS) secretion", *Diagnostics*, 9(4), 205 (2019).
34. S. Heebøll, K.L. Thomsen, A. Clouston, E.I. Sundelin, Y. Radko, L.P. Christensen, M. Ramezani-Moghadam, M. Kreutzfeldt, S.B. Pedersen, N. Jessen, L. Hebbard, J. George and H. Grønbaek, "Effect of resveratrol on experimental non-alcoholic steatohepatitis", *Pharmacol Res*, 95-96, 34-41 (2015).
35. S. Chen, X. Zhao, L. Ran, J. Wan, X. Wang, Y. Qin, F. Shu, Y. Gao, L. Yuan and Q. Zhang, "Resveratrol improves insulin resistance, glucose and lipid metabolism in patients with non-alcoholic fatty liver disease: a randomized controlled trial", *Dig Liver Dis*, 47, 226-232 (2015).
36. H. Wang, H. Wang, W. Yang, M. Yu, S. Sun and B. Xie, "Improved Oral Bioavailability and Liver Targeting of Sorafenib Solid Lipid Nanoparticles in Rats", *AAPS PharmSciTech*, 19(2), 761-768 (2018).



نشرة العلوم الصيدلانية جامعة أسيوط



إظهار نتائج واعدة على مرض الكبد الدهني غير الكحولي باستخدام صواعغات دهنية نانومترية تحتوي على ريسفيراترول

دينا عادل كامل^{١*} - بسمة ناجي عبد الحميد^١ - نورا حسن عبد اللاه^٢ - سيد إسماعيل محمد^١

^١ قسم الصيدلانيات، كلية الصيدلة، جامعة أسيوط، أسيوط، مصر

^٢ قسم الصيدلانيات، كلية الصيدلة، جامعة بدر بأسيوط، أسيوط، مصر

يؤثر انتشار مرض الكبد الدهني غير الكحولي (NAFLD) على أكثر من ٢٥٪ من السكان في جميع أنحاء العالم. تهدف الدراسة الحالية إلى صياغة الجسيمات النانومترية الدهنية الصلبة المحملة بالريسفيراترول (Res-SLNs) وتقييم المتغيرات التجريبية المختلفة. تم تحضير اثنين من Res-SLNs بطريقة الاستحلاب وتم تقييمهما في المختبر بقياسات معملية مختلفة. تم اختيار Res-SLN1 لمزيد من الدراسات المعملية. بعد ذلك، أجريت دراسات في الجسم الحي عن طريق أحداث مرض الكبد الدهني في الفئران عن طريق إعطائهم نظام غذائي يحتوي على نسبة عالية من الدهون (HF) لمدة ١٢ أسبوعاً تليها فترة ٦ أسابيع من العلاج باستخدام Res-SLN1. تم أخذ عينات الدم من الفئران لتقييم مستوى الدهون وأنزيمات الكبد. تمت معالجة أجزاء أخرى من الكبد للتقييمات النسيجية. أظهرت الصواعة النانومترية Res-SLN ١ كفاءة تحمل عالية تبلغ $75 \pm 22\%$ وحجم متناهي الصغر بمتوسط 208 ± 48 نانومتر. كشفت الصواعغات الدهنية النانومترية عن معدل مقبول فيما يخص الإنطلاق الدوائي المعملية. كان هناك تحسن ملحوظ في مستوى الدهون ومستويات إنزيمات الكبد عند إعطاء Res-SLN1 مقارنة بمجموعة HF التي لم تتلقى اي علاج. تظهر النتائج النسيجية في مجموعة HF تضخماً وتليفاً في نسيج الكبد الذي أظهر تحسناً عن طريق إعطاء Res-SLNs. لذلك، تمثل الصواعغات الدهنية النانومترية التي تحتوي على ريسفيراترول نهجاً علاجياً واعداً لمرض الكبد الدهني غير الكحولي.